Control of Cylinder Wake Using Three Dimensional Disturbances

S. Bhattacharya and A. Ahmed**
Department of Aerospace Engineering, Auburn University, Auburn, AL, USA, 36849

Abstract
Wake of a circular cylinder subjected to acoustically driven disturbances introduced from sinusoidal slits was investigated at Reynolds number of 24,000 and 40,000. Results showed that the amplitude of the primary shedding frequency was eliminated when the forcing frequency was twice the fundamental frequency. This is attributed to the mechanism of redistribution of energy from the large coherent structures to the smaller ones. Furthermore, the introduction of three dimensional disturbances accelerated the separating shear layers which narrowed the wake and made it uniform in terms of mean velocity and reduced drag.

1. INTRODUCTION

Flow around a bluff body remains one of the active areas of research in fluid dynamics due to its practical importance in aerodynamics, combustion, marine hydrodynamics etc. Bluff body flow control challenges broadly include the issues related to boundary layer separation and wake modification through changes in flow structure by different means. A review paper by Choi et al [1] summarizes the research work done so far in the area of flow control.

Vortex induced vibration of bluff bodies which may eventually trigger resonance and structural failure is primarily due to aerodynamic forces that are generated in the wake because of the periodic shedding of von Karman vortices [2-5]. In addition to the spanwise von Karman and Kelvin Helmholtz vortices, streamwise vortices are also present in the wake whose characteristics change with the Reynolds number [6]. The control of primary shedding and distribution of energy to smaller structures for effective dissipation therefore constitutes an important aspect of a wake flow control strategy.

Bluff body flow control schemes can be broadly categorized into two types; passive and active. Passive methods include modification of the body geometry or other surface characteristics such as surface roughness [7]. Few prominent methods under passive control include surface mounted helical wires [8], and splitter plates [9-10] etc. The primary motivation for the passive control is to disrupt the spanwise structure of the Karman vortex street by introducing spanwise disturbance. Numerical studies have also substantiated this aspect of the flow control [11].

Active control methods on the other hand use external forcing devices to introduce disturbances in the flow through steady blowing and suction [12], and synthetic jets [13] etc. It is possible to design feedback control system based on the output of some sensing elements in the flow field and then drive the forcing devices accordingly [10,14].

Acoustic forcing has been shown to be an effective mean of active control of a bluff body wake. Blevins [15] investigated the influence of sound waves on the vortex shedding from a circular cylinder for the range of Reynolds number (Re) between 20,000 and 40,000. His results showed that application of sound correlated the spanwise vortex shedding. This was confirmed by the signals obtained from four flush film sensors placed on different spanwise locations on the cylinder. In the absence of excitation the signals were incoherent and irregular. When acoustic signal with 143.5 dB sound pressure level was introduced at the shedding frequency, the four signals were nearly in phase with less irregularity. This showed that the application of acoustic excitation synchronized the frequency and was able to increase the strength of vortex shedding. Another important finding from this experiment was that the sound applied near vortex shedding frequency shifted vortex shedding to the forcing frequency.

By attaching speakers at the both end of a circular cylinder Hsiao and Shyu [16] introduced acoustic disturbances in the cylinder wake through a thin straight slit on the cylinder surface. They showed that the separated shear layers were sensitive to the excitation. When the frequency of the internal acoustic

**Corresponding author, email–bhattacharya.30@buckeyemail.osu.edu, ph no: 334 444 1674,

excitation was around the shear layer instability frequency the drag reduction was maximum accompanied by a marked reduction in the amplitude of the shedding frequency. The flow visualization also showed that the Karman vortex street was perturbed to form smaller vortices that significantly increased the three dimensionality of the wake.

In an experiment performed by Huang [17], pure tone sound was introduced in the flow field of a circular cylinder through a thin slit on the cylinder surface for the range of Reynolds number between 4,000 and 8,000. He found that vortex shedding was suppressed by the excitation however there was an optimum sound level for the maximum suppression. When the introduced disturbances had a measured sound level of 70 db at the slit, the natural shedding peak was almost eliminated at seven cylinder diameters downstream. He also showed that there was a very narrow bandwidth of excitation frequencies for which a noticeable suppression of the shedding was achievable.

Fujisawa et al., [18] performed similar experiments with acoustic excitation on a 50 mm diameter cylinder with aspect ratio of 8 at Reynolds number of 9,000. The drag coefficient calculated from the surface pressure distribution showed that it had a minimum for a slit angle of 90^o, and when the excitation frequency was 4 times the natural shedding frequency i.e. around the unstable frequency of the shear layer.

In a later study, Fujisawa et al., [19] investigated the effect of internal acoustic excitation at Reynolds number of 9,000 using phase averaged Particle Image Velocimetry (PIV). The phase averaged results showed the formation of discrete vortices along the shear layer of the cylinder wake when the excitation frequency was four times the vortex shedding frequency. They concluded that due to the interaction of the vortices with the wake the velocity fluctuation in the flow field was weakened.

It may be noted that most of the above mentioned studies were conducted at Reynolds numbers below 10,000. In the investigation reported by Hsiao and Shyu the Reynolds number was 20,000. To the author's knowledge except this work, there has been no attempt to investigate the effect of acoustic disturbances in the wake of a circular cylinder at a higher Reynolds number range.

The flow over a cylinder at higher Reynolds number contains multiple global modes among which the Karman shedding is the first mode to become unstable. So whether internal acoustic excitation is successful in suppressing the shedding component and how exactly it influences the turbulent wake is worthwhile to investigate. Another important difference of the present work with the previous research is the geometry of the slit. All the research done so far, have used a straight slit which essentially introduce a two dimensional disturbance. Therefore an introduction of a three dimensional disturbance through a wavy slit, was thought to be more effective. The primary objective of this work was to investigate the influence of three dimensional disturbances of different frequencies on the turbulent wake of a circular cylinder and the understanding of the mechanism of drag reduction.

2. EXPERIMENTAL SETUP

2.1. Cylinder Model

For the flow control experiment, copper cylinders of 41.3 mm outer diameter, thickness 1 mm and length 203 mm were used. Two sinusoidal slits of 0.5 mm width and 60 mm wavelength (λ) were made by laser cutting operation, on two diametrically opposite locations on the surface of the cylinder (fig. 1). The peak to peak amplitude of the slit (A = 10 mm) was selected such that it remained within 80 deg and 100 deg azimuthally on the surface.

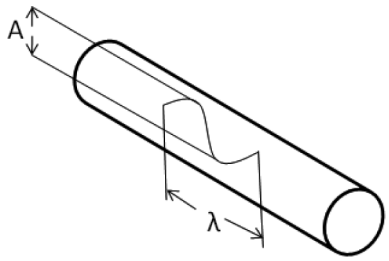

Figure 1. Description of the sinusoidal slits on model surface.

2.2. Acoustic Driver

The test cylinder was supported on both the sides by two elliptical end plates to maintain the two dimensional flow over the cylinder. The acoustic excitation was provided by two subwoofers of

maximum input power of 300W, attached to the both end of the cylinder (fig. 2). A LabView program was used to generate sinusoidal signal of desired frequencies for driving the speakers. NI PCI-6035E DAQ board was used for all signal generation and data acquisition and the signal was amplified by a power amplifier to drive the speakers.

2.3. Choice of Slit Length

The experiment was modeled to compare results with Hsiao's (1991) straight slit work (slit of length 8 cm on a 25 cm long cylinder with an aspect ratio 4.1). For the present experiment the length of the slit was selected based on the requirement to avoid presence of nodes at the slit due to standing waves (Resonant tube theory). In designing the experiment, position of up to four nodes was calculated for various cylinder lengths and diameters and it was found that the above length of slit and cylinder diameter was adequate in preventing asymmetric flow conditions at the slit due to acoustic loading. Another advantage of using a short slit instead of a slit spanning the whole length of the cylinder is the uniformity of the forcing. It was difficult to obtain satisfactory blowing from a longer slit with the speaker and amplifier setup used in this experiment since the combination of periodic forcing, mass displacement requirements and cavity impedance imposed additional limitations on the driver.

2.4. Wind Tunnel

The experiments were conducted in the 3ft X 4ft cross section closed return wind tunnel of Auburn University. The non uniformity of the flow was found to be 1% and the free stream turbulence level was 0.5%. For the test setup the maximum test section blockage ratio was 0.045. Experiments were conducted at two different speeds of the tunnel, 9 m/sec and 15 m/sec resulting in Reynolds number of 24,000 and 40,000 based on the diameter of the cylinder. The cylinder wake was surveyed up to 10 diameters downstream at a stream wise spacing of 1 diameter. A two axis traverse system was used for the vertical and horizontal movement of the hot wire probes. The traverse controller was programmed by a Labview code for automatic traversing and was connected to the main computer through serial ports.

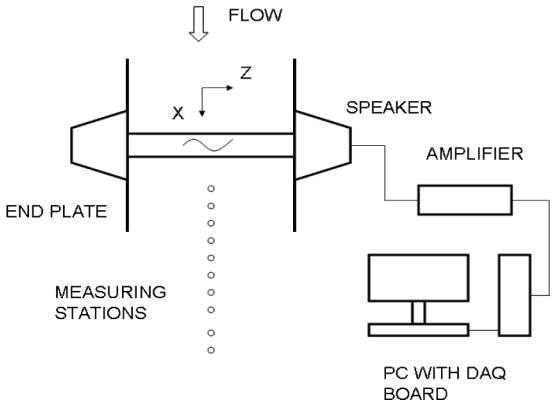

Figure 2. Experimental set-up in the wind tunnel.

2.5. Hot Wire Measurements

The energy spectra of the fluctuating velocities and the blowing coefficient for the acoustic excitation were obtained by a single wire (Dantec P15). The turbulent quantities in the wake were measured with Dantec 55P61 X-wire probes of 5 μm wire diameter and 1.25 mm prong separation. To properly identify the shear layer for spectral measurement the signal from the hotwire was constantly monitored on a HITACHI oscilloscope. The hot wire signals were sampled using NI PCI-6035E DAQ board. Both the single wire and the X wire probes were calibrated in-situ in the wind tunnel before each run. The transfer function for calibration curve was obtained by using a fourth order polynomial fitting to the measured voltage and velocity of the tunnel. Data was sampled at 4 kHz and a total of 12 K samples were collected at each measuring point. The sampled data were post processed using Matlab software.

2.6. Drag Measurement

In addition to the hotwire anemometry, total pressures in the wake were measured by using a pitot tube which was connected to a Validyne DP 45-14 differential pressure transducer. The signal from the transducer was conditioned using a Validyne, CD 12 carrier demodulator. The drag was computed by numerically calculating the momentum thickness. The drag coefficient C_d is defined as

$$C_d = \frac{2\theta}{d} \tag{1}$$

Where θ is the momentum thickness which was obtained by numerically integrating the wake velocity profiles using the relationship,

$$\theta = \int \frac{u}{U_\infty}\left(1 - \frac{u}{U_\infty}\right) dy \tag{2}$$

2.7. Uncertainty Measurement

In order to quantify the experimental uncertainties involved with a hot wire measurement, uncertainty calculations were carried out in accordance with the method prescribed in [20]. The reference case selected for the uncertainty evaluation was that of Reynolds number of 24,000. The uncertainties involved in the calculation of mean velocity profiles are addressed here. For calculation of uncertainty the following sources of error were considered (uncertainty due to temperature and pressure variation during measurement was ignored).

- Pressure transducer error
- Pressure transducer calibration error
- Hot wire calibration error
- A/D board resolution error

Table 1 shows the various uncertainties. The total uncertainty involved in the hot wire measurement was found to be 2.83%.

Table 1. Uncertainties for hot wire measurement.

Error Source	Value	Coverage Factor	Relative Standard Uncertainty
Calibrator	0.02	2	0.01
Pressure transducer calibration	0.02	2	0.01
Hot wire calibration	0.0014	2	0.0007
A/D board resolution	0.0013	1.732	0.0002

2.8. Water Tunnel Flow Visualization

Limited flow visualization experiments were conducted in the Auburn University 45 cm X 45 cm water tunnel. The set up for water tunnel flow visualization was different from that of the wind tunnel (fig 3). The same cylinder model was placed vertically in the water tunnel with the submerged bottom end sealed properly. The top end was attached to the driver enclosure. A dye port allowed supply of fluorescent dye inside cavity of the cylinder. A laser sheet was created tangentially on the cylinder surface using a 4 w argon-ion laser beam. Video images from a Panasonic video camera were recorded on a Toshiba SV-F990 VCR. Video records were analyzed frame by frame and selected images were printed. The purpose of the flow visualization study was to get a qualitative picture of the flow emanating from the sinusoidal slit.

3. RESULTS AND DISCUSSIONS

3.1. Blowing Coefficient

The cylinder was placed in between the end plates in such a way so that the mean axis of the sinusoidal slit on the top surface was at 90 degree from the attachment line. The blowing coefficient ($C\mu$) for each case was calculated as $C_\mu = v_s / U_\infty$, where v_s is the disturbance velocity from the slit in the absence of free stream velocity.

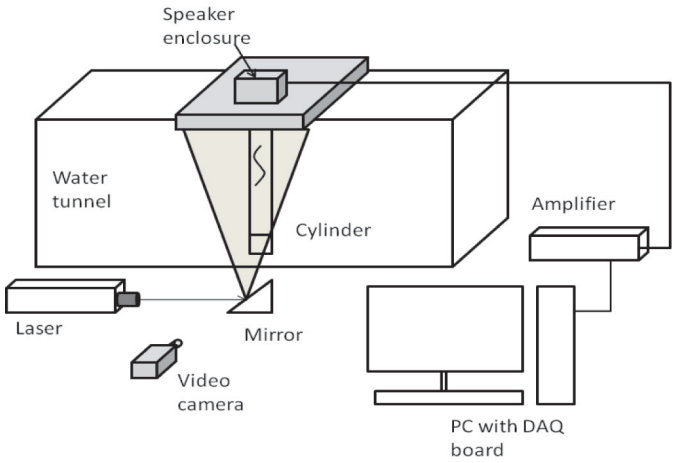

Figure 3. Experimental set-up for flow visualization in water tunnel.

Table 2. Blowing coefficients for different forcing frequencies.

Re = 24,000		Re = 40,000	
Forcing frequency (Hz)	**Cμ**	**Forcing frequency (Hz)**	**Cμ**
25	0.23	38	0.13
50	0.23	76	0.13
100	0.23	152	0.13
180	0.23	180	0.13

Variation of the blowing coefficient was limited due to two factors, driver power requirement and level of blowing through the slit. It was found that blowing coefficients below these values were not effective in introducing sufficient forcing. It may be noted that this investigation did not focus on the effect of different blowing strengths.

3.2. Effect of Excitation on Vortex Shedding

A single wire was placed in the upper shear layer zone (y/d = 0.5, x/d = 1) to measure the vortex shedding frequency (fs_0) and was found to be 50 Hz and 76 Hz for Reynolds numbers of 24,000 and 40,000 respectively. The acoustic driver was operated with a number of different frequencies with the maximum being 180 Hz. It was not feasible to operate the driver at higher frequencies as it adversely affected the amplitude. For this reason, for the higher Reynolds number case the frequency of 310 Hz ($4\ fs_0$) was not selected as it was found that at this frequency the blowing coefficient was not sufficient for the experiment.

Figure 4 shows the wake power spectra for different forcing frequencies at Re of 24,000. For this case, forcing at a frequency almost close to the shedding frequency did not have any considerable effect on the Karman shedding, as evident from the comparable height of the peaks in the spectrum plot in the two cases. When the forcing frequency was $fs_0/2$ a distinct peak appeared in the sub-harmonic side of the spectrum. In the case of forcing at $2fs_0$ the shedding peak disappeared completely. This was also observed when the forcing frequency was 180 Hz. The complete cancellation of shedding peak was not observed when the forcing frequency was below 100 Hz at this Reynolds number.

At higher Reynolds number (40,000), the power spectrum shows that in the event of excitation with a frequency almost equal to the shedding frequency the shedding peak got considerably strengthened (fig.5). When the forcing frequency was $fs_0/2$ (sub-harmonic forcing) a distinct peak appeared in this range. In case of excitation at $2fs_0$ the shedding peak disappeared. The shedding peak remained cancelled when higher excitation frequency of 180 Hz was applied.

From the spectrum plots discussed so far it is clear that when the forcing frequency was twice the shedding frequency the acoustic excitation successfully eliminated the shedding peak completely. Except Huang's work [17] where he reported to have eliminated the shedding peak with a acoustic excitation of same frequency at a downstream distance greater than x/d = 7, all the other research done with internal

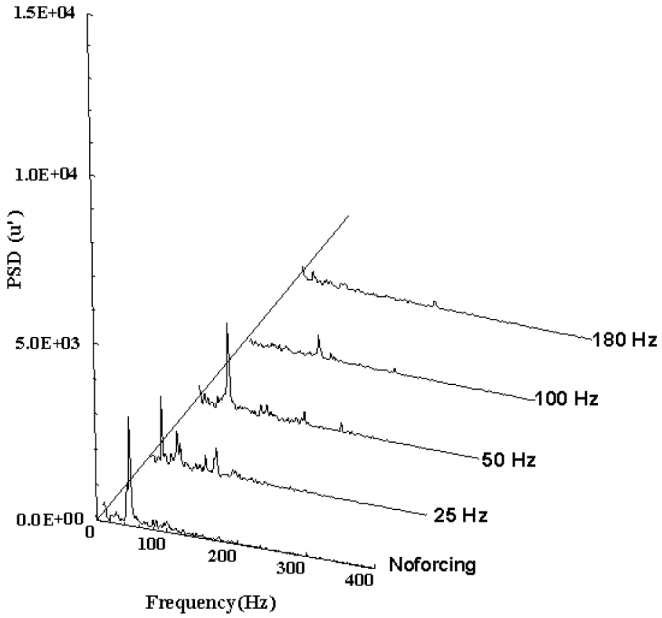

Figure 4. Energy spectra for different forcing frequencies, x/d = 1, y/d = 0.5, Re = 24,000.

acoustic excitation have shown that in the low Reynolds number range, a forcing frequency which was around four times the shedding frequency was necessary to neutralize the vortex shedding completely. Hsiao et al [16] showed that only when the forcing frequency was at least of the order of the shear layer instability frequency, excitation was able to eliminate the shedding. However in the present work, elimination of shedding peak was achieved with a forcing frequency much below the shear layer instability frequency. Also the disturbances introduced in the flow through a sinusoidal slit were highly three-dimensional that consequently increased the perturbations in the flow. That is, the mechanism of cancellation of shedding can be attributed to the degree of three dimensionality introduced which in turn depend on the slit geometry, blowing coefficient and the frequency of excitation. Furthermore, it is possible to achieve cancellation of shedding peak even with an excitation of frequency less than the shear layer instability frequency provided the blowing coefficient or in other words the amplitude of excitation is high and the resultant three dimensionality introduced is effective in disrupting the shedding pattern. This argument supports the flow visualization study done by Hsiao et al [16] where it was shown that the basic mechanism for cancellation of shedding was the destruction of Karman vortices into smaller eddies near the cylinder.

Regarding the use of the parameter which aptly describes the effectiveness of forcing, it is suggested that blowing coefficient is a better term to use than sound pressure level as used by previous researchers. The excitation created by the speaker diaphragm forces a jet out of the slit, into the flow. It is not the acoustics rather the amplitude and frequency of the jet which is important for effective shedding control. Additionally, acoustics depend not only on the signal input but also on the material used in model construction, internal cavity resonance due to standing waves etc.

3.3. Effect of Excitation on Mean Velocity Distribution

Figure 6 illustrates the effect of forcing with 180 Hz excitation on the mean velocity profiles for the two Reynolds numbers. Due to the forcing, the upper and lower shear layers are accelerated. This acceleration is evident in the presence of a large velocity gradient around the region y/d = ±1. This increase in velocity of the free shear layers effectively narrows down the wake thus making the region more uniform in terms of flow velocity. Apart from the clear indication of a narrowing wake, figure 6 (a) also shows that up to about x/d = 4, the velocity of flow in the centerline of the wake has in fact came down in the case of forcing with 180 Hz excitation for Re of 24,000. This trend was not visible after wards. From x/d = 6 to x/d = 10 the velocity profiles for the forcing case maintains the accelerating character of the shear layers and more uniform velocity profiles, thus indicating lower value of momentum loss from the no forcing case, which ultimately contribute to lower drag.

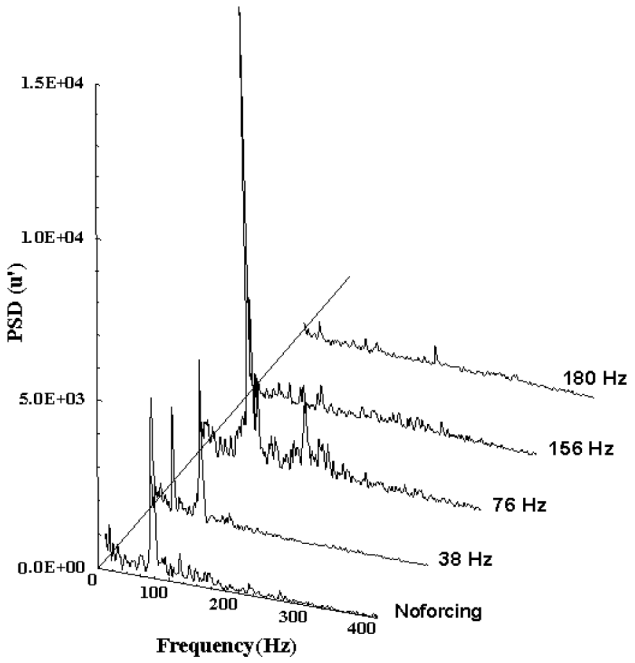

Figure 5. Energy spectra for different forcing frequencies, x/d = 1, y/d = 0.5, Re = 40,000.

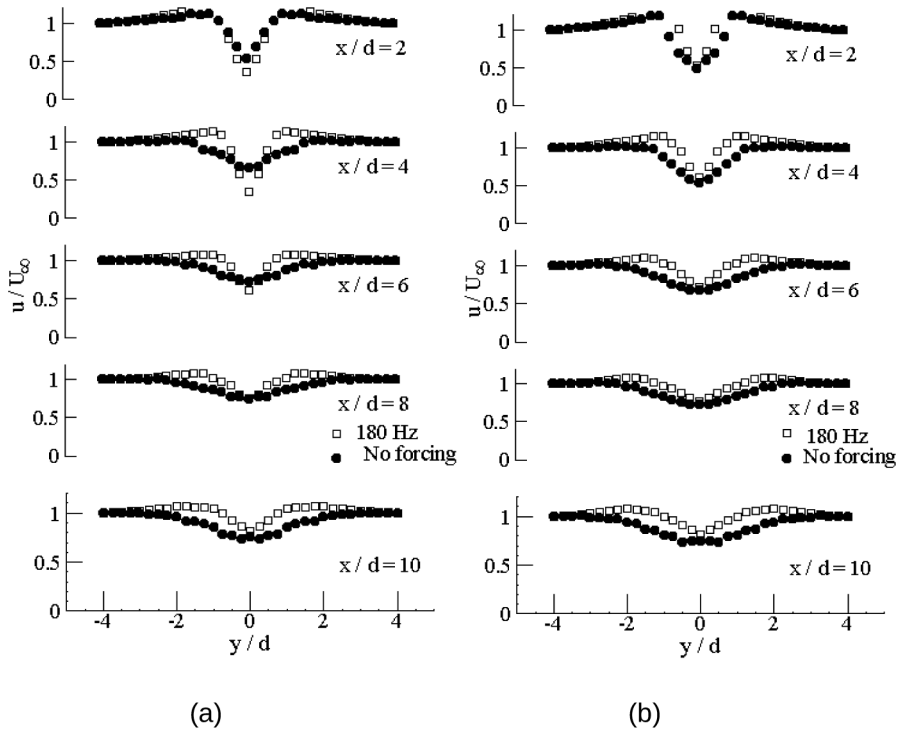

Figure 6. Cross sectional distribution of mean velocity, (a) Re = 24,000 (b) Re = 40,000.

Table 3. Drag coefficients for different forcing frequencies.

Re = 24,000		**Re = 40,000**	
Excitation frequency (Hz)	**C_d**	**Excitation frequency (Hz)**	**C_d**
No Forcing	1.13	No Forcing	1.20
50	1.08	76	1.02
180	0.56	180	0.84

The drag coefficients computed from the mean velocity profiles at x/d = 10 (measured by pitot tube) are presented in Table 3.

It is interesting to note that at Re of 24,000, the drag reduction was almost 50 % compared to 30 % in case of Re of 40,000.

To determine the effect of forcing on the evolution of the wake the half wake width was determined from the mean velocity profiles. The half wake width δ is defined as the distance of the location from the center of the wake where the velocity defect is half the maximum velocity defect. From figure 7 it is evident that forcing resulted in narrower wake for both cases.

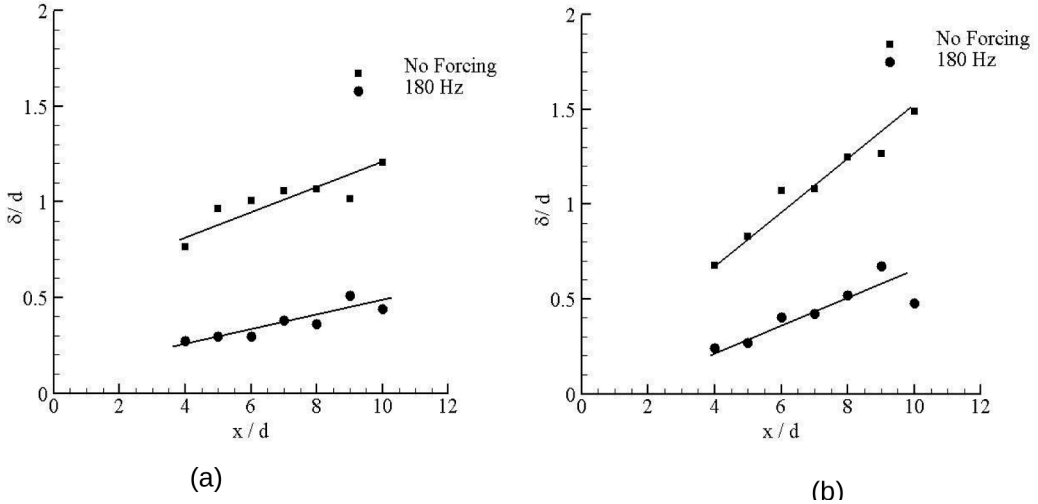

Figure 7. Variation of half wake width (a) Re = 24,000 (b) Re = 40,000.

3.4. Effect of Excitation on Fluctuating Quantities

The cross sectional distribution of velocity fluctuations in the wake of the circular cylinder is shown in figure 8 and 9, where the results under acoustic forcing have been compared with that of no forcing case. Representative plots for x/d = 2 to x/d = 10 have been included. The normal and streamwise velocity fluctuations , u' and, v', are mostly reduced by the application of forcing in lower Reynolds

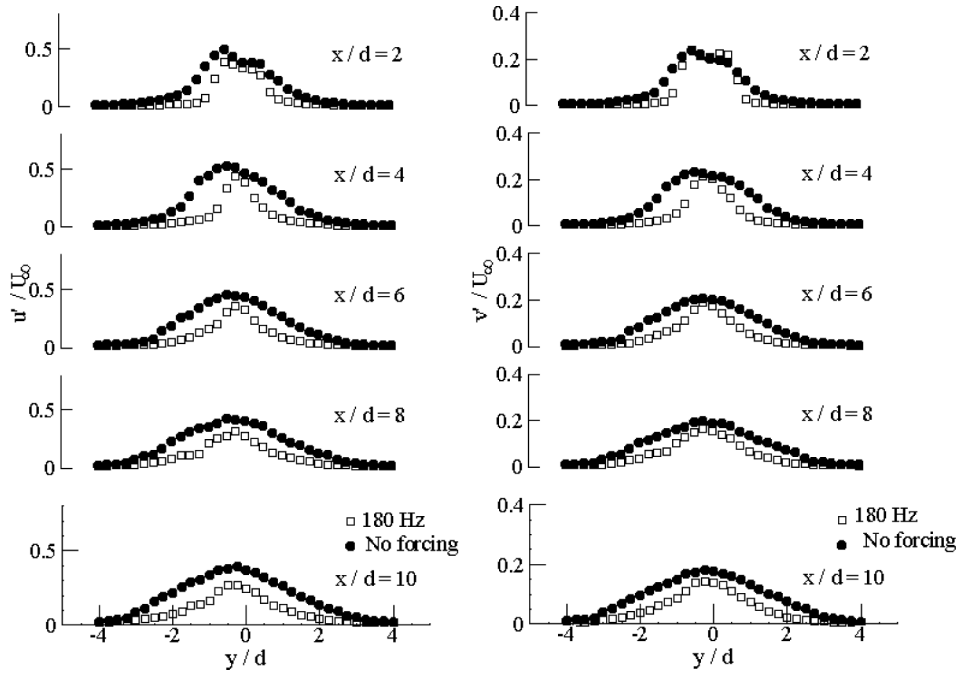

Figure 8. Cross sectional distribution of velocity fluctuation, u' and v', Re = 24,000.

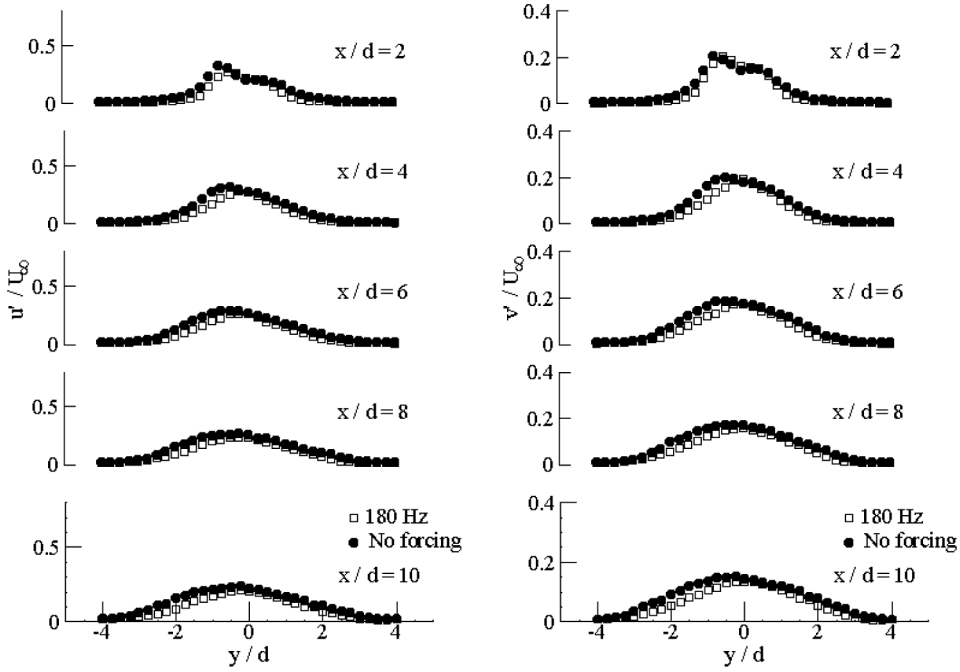

Figure 9. Cross sectional distribution of velocity fluctuation, u' and, v' Re = 40,000.

number case. This is attributed to the appearance of a more uniform wake in the case of forcing. At all streamwise positions the suppression of fluctuation is evident in case of 180 Hz forcing. However this suppression is not strong in the higher Reynolds number case as seen from figure 9. Due to the high flow velocity in this case the magnitude of the forcing disturbance is not that effective in suppressing the velocity fluctuation compared to the low Reynolds number case. The success of forcing with 180 Hz at lower Reynolds number case can also be explained in terms of the non-dimensionalised Strouhal number. It is to be noted that the natural Strouhal number of the low Reynolds number case was 0.23 (for shedding frequency of 50 Hz) and for the other case it was 0.21(for shedding frequency of 76 Hz). And for a forcing frequency of 180 Hz, we get the Strouhal number of forcing as 0.86 in the low Re case compared to 0.49 for the higher Re case. Since the non dimensional Strouhal number of the forcing is almost double in the lower Re case, it was more effective in suppressing fluctuation.

3.5. Distribution of Energy in the Shedding Peak in the Spectrum

The single wire sensor was traversed vertically at 0.25d spacing from y/d = ±4. This was repeated for each streamwise location (from x/d = 1 to x/d = 10) resulting in a data grid consisting of 330 points. The spectrum plot was obtained from the time series signal obtained by the hot wire sensor at each of the data point in the wake. The maximum power within a small frequency band in the spectra (corresponding to shedding frequency ± 5 Hz) was later determined. Since shedding frequency has the longest peak in that band, the maximum value can be safely assumed to represent power in shedding peak. This data was used to plot the contours as shown in figure 10 and 11. The contour plot signifies the distribution of energy in the shedding component in the entire wake up to x /d = 10. This distribution is useful in determining how the vortical structures develop in the near wake of a circular cylinder under forcing compared to that of no forcing case. In the no forcing case, maximum energy was contained in the two shear layers emanating from the top and bottom sides of the cylinder i.e. around y/d = ±0.5 and extended to x/d = 2. This was the region where spectrum of the hot wire signal registered strongest peaks of the vortex shedding frequency. In the center of the wake as two vortices from the top and bottom side of the cylinder curl in, the peak in the spectrum plot shifted to $2fs_0$. Gradually these structures convected downstream and simultaneously the energy content of the shedding component reduced that indicated the distribution of the energy to smaller scales. On the other hand, the introduction of the forcing with 180 Hz excitation, through the top and bottom slit of the circular cylinder had some remarkable effect on the wake. From figure 11 it is evident the energy level in the main shedding component was considerably reduced. The maximum values were not localized around

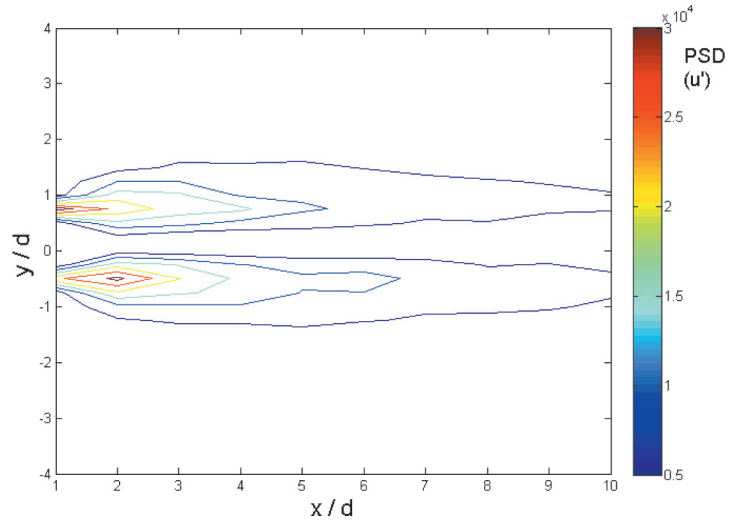

Figure 10. Contour plot of the magnitude of the shedding peak without forcing, Re = 24,000.

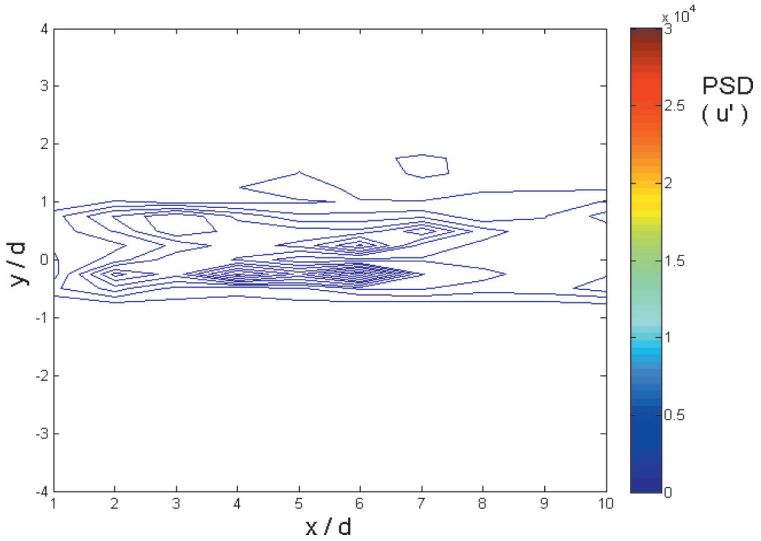

Figure 11. Contour plot of the magnitude of the shedding peak with 180 Hz forcing, Re = 24,000.

the separating shear layer anymore; rather they were distributed in the wake in a uniform manner. Also the wake became narrower as indicated by the vertical width of the contour plot. This is attributed to the disturbance introduced in the flow through the sinusoidal slits which inhibited the regular development of the vortices from the two sides and resulted in smaller scales. Moreover these smaller eddies carried less energy downstream than the bigger eddies. Along with this as the uniformity in the flow velocity increased, the wake narrowed down further downstream and contributed to the suppression of the normal and stream wise velocity fluctuations.

3.6. Flow Visualization

To further investigate the interaction of the flow from the slit with the surrounding limited flow visualization was conducted in the water tunnel. The figure below shows the structure of the flow emanating from the slit. As clearly seen the flow from the slit contains small scale vortices which are being introduced in the surrounding flow. This introduction of smaller scale structures disrupt the formation of regular vortex street as explained earlier. The degree of three-dimensionality is also notable due to the presence of a sinusoidal slit (Figure 12a). Figure 12b shows periodic structures similar to a synthetic jet [13].

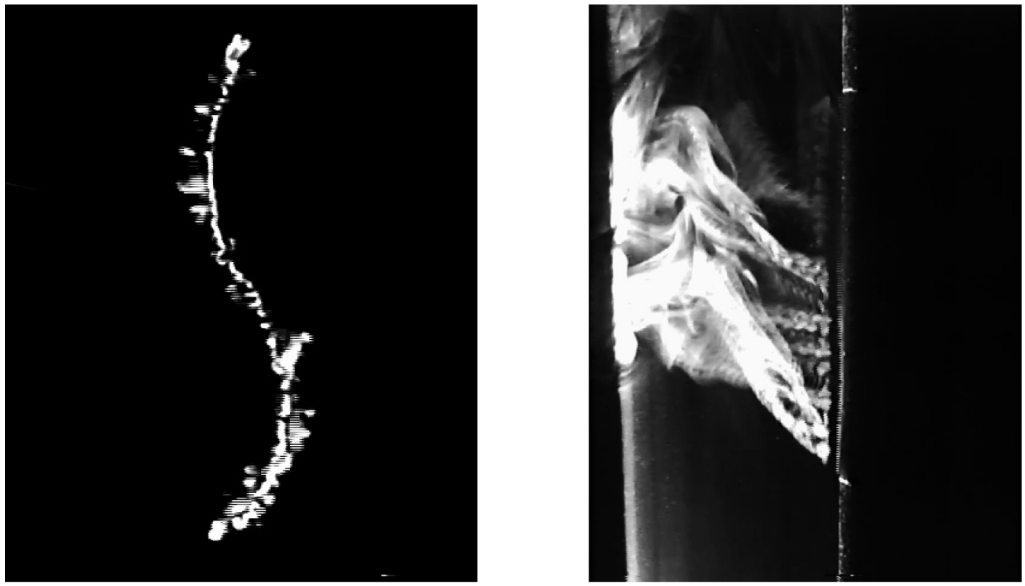

(a) (b)

Figure 12. Flow visualization in water tunnel.

4. CONCLUSION

The wake of a circular cylinder was investigated with a three dimensional disturbances introduced in the flow field through two sinusoidal slits located on two diametrically opposite sides of the cylinder. For Reynolds number 24,000 case a forcing frequency that was twice the fundamental shedding frequency was able to eliminate the shedding peak completely. Results for the Reynolds number 40,000 were similar however disturbances introduced at the fundamental frequency amplified the primary instability. The mean velocity plot showed that the wake width narrowed considerably due to forcing that accelerated the shear layers and reduced drag. It is further concluded that forcing frequency that is less than four times the shedding frequency can eliminate the shedding peak in a turbulent wake of a circular cylinder provided the blowing coefficient and slit geometry synergistically create three dimensional disturbances that effectively distribute energy from larger structures to the smaller eddies.

REFERENCES

[1] H. Choi, WP. Jeon, J. Kim, "Control of Flow Over Bluff Body", Annual Review of Fluid Mechanics, Vol. 40, 2008, 113–139.

[2] R. King, "A Review of Vortex Shedding Research And Its Application", Ocean Engineering, Vol. 4, 1977, 141–152.

[3] R.E.D. Bishop, A.Y. Hassan, "The Lift and Drag Forces on a Circular Cylinder in a Flowing Fluid", Proceedings Royal Society (London), Series A 277, 1964, 32–50.

[4] R.D. Blevins, Flow Induced Vibration, 2nd edition, 1990. Van Nostrand Reinhold, NY.

[5] Y. C. Fung, "Fluctuating Lift and Drag Acting on a Cylinder in a Flow at Supercritical Reynolds Numbers", Journal of Aerospace Sciences Vol. 24, 1960, 801–804.

[6] Bays-Muchmore, B., and Ahmed, A., "On the Streamwise Vortices in the Turbulent Wakes of Cylinders," Physics of Fluids A, Vol. 5, No. 2, pp 387–392, 1993.

[7] WCL. Shih, C. Wang, D. Coles, A. Roshko, "Experiments On Flow Past Rough Circular Cylinders At Large Reynolds Numbers", Journal of Wind Engineering and Industrial Aerodynamics. Vol. 49, 1993, 351–368.

[8] S. Lee, H. Kim, "The Effect of Surface Protrusions on the Near Wake of A Circular Cylinder", Journal of Wind Engineering and Industrial Aerodynamics, Vol. 69-71, 1997, 351–361.

[9] P.W. Bearman, "Investigation of the Flow Behind A Two – Dimensional Model with A Blunt Trailing Edge and Fitted With Splitter Plates", Journal of Fluid Mechanics Vol. 21, 1965, 241–255.

[10] M.J. Khan, A. Ahmed, "Sub-Harmonic and Harmonic Response of the Wake of A Circular Cylinder", AIAA Journal, Vol. 31, 1993, 208–209.

[11] R.M Darekar, S.J Sherwin., "Flow Past A Square -Section Cylinder with A Wavy Stagnation Face", Journal of Fluid Mechanics Vol. 426, 2001, 263–295.

[12] D. Arcas, L. Redekopp, "Aspects Of Wake Vortex Control Through Base Blowing/Suction", Physics of Fluids, Vol. 16, 2004, 452–456.

[13] M. Amitay, BL. Smith, A. Glezer, "Aerodynamic Flow Control Using Synthetic Jet Technology", 36th AIAA Aerospace Science Meeting, Reno Nevada, AIAA paper no 98–0208.

[14] M.D. Gunzburger, H.C. Lee, "Feedback Control of Karman Vortex Shedding", ASME Journal of Applied Mechanics, Vol. 63, 1996, 828–835.

[15] R.D. Blevins, "The Effect Of Sound On Vortex Shedding From Cylinders", Journal of Fluid Mechanics, Vol. 161, 1985, 215–237.

[16] F.B. Hsiao, J.Y Shyu, "Influence Of Internal Acoustic Excitation Upon Flow Passing A Circular Cylinder", Journal of Fluids and Structures, Vol. 5, 1991, 427–442.

[17] X.Y. Huang, "Suppression Of Vortex Shedding From A Circular Cylinder By Internal Acoustic Excitation", Journal of Fluids and Structures, Vol. 9, 1995, 563–570.

[18] N. Fujisawa, G. Takeda, "Flow Control Around A Circular Cylinder By Internal Acoustic Excitation", Journal of Fluids and Structures, Vol. 15, 2003, 903–913.

[19] N. Fujisawa, G. Takeda, N. Ike, "Phase Averaged Characteristics of Flow Around a Circular Cylinder Under Acoustic Excitation Control", Journal of Fluids and Structures, Vol. 19, 2004, 159–150.

[20] F.E. JØrgensen, "How to Measure Turbulence with Hot Wire Anemometers-a Practical Guide", 2002, Dantec Dynamics.